

The role of slow magnetostrophic waves in dipole formation in rapidly rotating dynamos

Aditya Varma and Binod Sreenivasan

26-04-2021

Indian Institute of Science, Bangalore, India

- Earth's magnetic field is predominantly an axial dipole.
- It is generated by dynamo action in the Earth's core.
- The driving force for the dynamo is a combination of thermal and compositional convection.
- Studies such as Sreenivasan and Jones (2011) and Sreenivasan and Kar (2018) indicate the importance of growth of kinetic helicity in the generation and sustenance of dipole.
- Ranjan and Davidson (2018) highlight the importance of inertial waves in segregation and distribution of helicity in dynamo systems.

Objective of study

- To study the growth of a small intensity 'seed' dipole field to form a large scale dipole field.
- Comparison of the dynamics involved in the formation of a dipole for a nonlinear and kinematic (where Lorentz force is ignored in the momentum equation) dynamo.
- Exploration of a wave mechanism in the formation of a dipole in nonlinear dynamos.

Governing equations

The non-dimensional governing equations are given as follows

$$\frac{E}{Pm} \left(\frac{\partial \mathbf{u}}{\partial t} + (\nabla \times \mathbf{u}) \times \mathbf{u} \right) + \hat{\mathbf{z}} \times \mathbf{u} = -\nabla p^* + (\nabla \times \mathbf{B}) \times \mathbf{B} + qRaTr + E\nabla^2 \mathbf{u} \quad (1)$$

$$\frac{\partial T}{\partial t} + (\mathbf{u} \cdot \nabla) T = q\nabla^2 T \quad (2)$$

$$\frac{\partial \mathbf{B}}{\partial t} = \nabla \times (\mathbf{u} \times \mathbf{B}) + \nabla^2 \mathbf{B} \quad (3)$$

$$\nabla \cdot \mathbf{u} = \nabla \cdot \mathbf{B} = 0 \quad (4)$$

Symbols

| Symbol | Quantity | Parameter | Definition |
|--------------|----------------------------|-----------|----------------------------------|
| u | Velocity | Pr | ν/κ |
| T | Temperature | Pm | ν/η |
| B | Magnetic field | q | κ/ν |
| j | Current density | E | $\nu/2\Omega L^2$ |
| ∇p^* | Modified pressure gradient | Ra | $g\alpha\Delta TL/2\Omega\kappa$ |
| | | Λ | $B_0/\sqrt{2\Omega\mu\rho\eta}$ |

Results

(a)

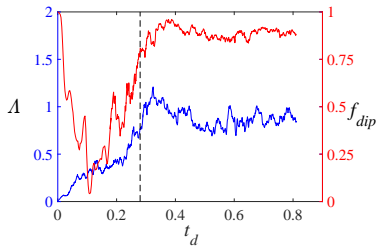


Figure 1: Evolution in time (measured in units of magnetic diffusion time) of the magnetic field strength given by the Elsasser number (Λ) and f_{dip} (measure of the dipole strength). The time at which the dipole is formed is indicated by a thin dashed black line in the plots.

- Simulation starts with a seed field of $\Lambda = 0.01$.
- The dipolar character is initially lost during the growth of the field and regain their dipole character at a later time. For parameters $Ra = 400$, $E = 1.2 \times 10^{-6}$, $Pm = Pr = 1$, dipole forms at $t_d = 0.28$.
- Magnetic field saturation occurs after $t_d = 0.35$ for $Ra = 400$.

Evolution of u_z

(a)

$Ra = 400, E = 1.2 \times 10^{-6}, Pm = Pr = 1$

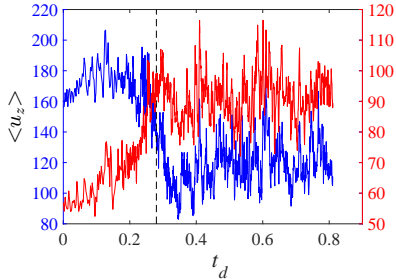


Figure 2: Root mean square value of u_z for two ranges of spherical harmonic degree $l \leq 30$ (red) and $l > 30$ (blue) in a dynamo simulation studying growth of seed field. The parameters are $Ra = 400$, $E = 1.2 \times 10^{-6}$, $Pm = Pr = 1$.

- Increase of magnetic field intensity is accompanied by an increase of the convective velocity u_z in the energy containing scales.
- Energy is extracted from scales smaller than the energy injection scale.
- Wave excitation is responsible for the excitation of convection in the large scales.

MAC force balance

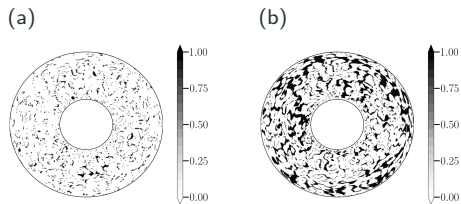


Figure 3: (a) and (b): Sections at $z = 0.1$ showing black patches where Lorentz force and Coriolis force (a) and buoyancy force and Coriolis force (b) are balancing each other respectively in the z -vorticity equation for $l \leq 30$. Parameters are $Ra = 400$, $q = 1$, $E = 1.2 \times 10^{-6}$.

- The generation of helicity requires a (Sreenivasan and Jones, 2011) balance between the Lorentz, Coriolis and buoyancy forces.
- Coriolis and buoyancy force balance each other in large parts of the shell.
- Where magnetic field is strong, the Lorentz force can balance the other two forces. Here, slow MAC waves can be produced.

MAC waves

MAC waves can be broadly classified in two: fast (high frequency) and slow waves (low frequency).

The frequencies are obtained as the roots by solving for the dispersion relation:

$$(\omega^2 - \omega_M^2 - \omega_A^2)(\omega^2 - \omega_M^2) - \omega_C^2 \omega^2 = 0 \quad (5)$$

2 sets of roots are obtained corresponding to the fast and slow waves.

The non-dimensional fundamental frequencies are as follows:

$$\begin{aligned} \omega_C^2 &= \bar{k}_z^2 / (\bar{k}^2 E_m^2), \\ \omega_A^2 &= qRa(\bar{k}_z^2 + \bar{m}^2) / \bar{k}^2 E_m, \\ \omega_M^2 &= (B_o \cdot \bar{k})^2 / E_m \end{aligned} \quad (6)$$

Frequency diagram

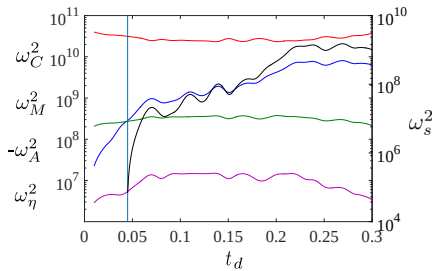
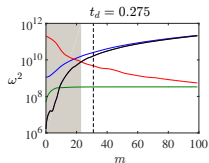


Figure 4: Fundamental frequencies plotted against time for the flow field for the scales $l < 30$. ω_m^2 -blue, ω_c^2 -red, ω_s^2 -black, $-\omega_a^2$ -green ω_η^2 -magenta respectively. The vertical indicates time at which slow wave frequency becomes real. Slow waves are excited at time $t_d = 0.047$. The parameters are $Ra = 400$, $q = 1$, $E = 1.2 \times 10^{-6}$, $Pm = Pr = 1$.

- Slow MAC waves are excited only when the Alfvén frequency exceeds the buoyancy frequency.
- This happens when the magnetic field has grown to sufficient strength to excite these waves and cause a helicity growth.
- Fast waves are excited from early times also, but there is not much helicity growth at these times.

Dipole contribution

(a)



(b)

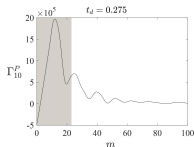


Figure 5: (a): Fundamental frequencies plotted against azimuthal wave-number m at $t_d = 0.275$. ω_c^2 -red, ω_m^2 -blue, $-\omega_a^2$ -yellow, ω_s^2 -black respectively. The shaded area shows the scales where helicity is generated. (b): Contribution to the dipole given by $\int B_{10}^P \cdot (\nabla \times (u \times B))$ plotted as a function of wavenumber m .

- The scales at which helicity is generated correspond to that of scales where slow MAC waves are excited and are distinct from fast waves (i.e. when $\omega_m < \omega_c$).
- Dipole contribution given by $\int B_{10}^P \cdot (\nabla \times (u \times B))$ (Buffet and Bloxham, 2002) occurs over the scales at which helicity is excited over the non-magnetic state.

Group velocity measurements

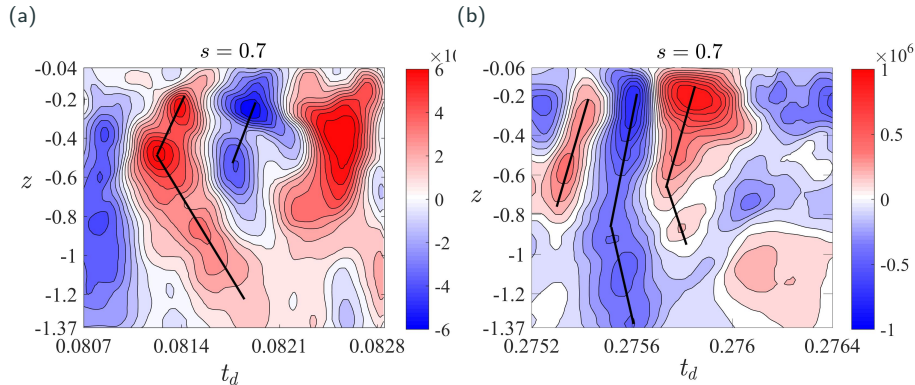


Figure 6: (a): Contour plots of \dot{u}_z for the time interval $t_d = 0.08 - 0.085$ (a) for the scales $l < 39$ and $25 < m < 38$. (b): Contour plots of \dot{u}_z for the time interval $t_d = 0.274 - 0.276$ (a)-(b) for the scales $l < 31$ and $m < 23$. The scales where helicity is generated is chosen for the group velocity measurements. The group velocity measurements: 1050 (a) and 4864 (b) matches closely with the estimated group velocity: 1257 (a) 4388 (b).

Conclusion

- Growth of kinetic helicity is due to slow MAC waves which are excited as the magnetic field grows in strength.
- Peak dipolar contribution occurs at scales which match with those at which helicity is generated.
- In kinematic dynamo simulations, only inertial waves are present. They are not enough to support the dipole.
- In nonlinear dynamo simulations, both slow and fast waves are present.
- The timescale of growth of convection and formation of dipole points towards importance of slow waves in forming dipole.

References

- Buffett, B. Bloxham, J., 2002. Energetics of numerical geodynamo models, *Geophysical journal international*, 149(1), 211–224.
- Davidson, P. A. Ranjan, A., 2018. On the spatial segregation of helicity by inertial waves in dynamo simulations and planetary cores, *Journal of Fluid Mechanics*, 851, 268–287.
- Sreenivasan, B. Jones, C. A., 2011. Helicity generation and subcritical behaviour in rapidly rotating dynamos, *Journal of Fluid Mechanics*, 688, 5–30.
- Sreenivasan, B. Kar, S., 2018. Scale dependence of kinetic helicity and selection of the axial dipole in rapidly rotating dynamos, *Physical Review Fluids*, 3(9), 093801